Simultaneous stimulated Raman scattering second harmonic generation in periodically poled lithium niobate

Gail McConnell
Centre for Biophotonics, Strathclyde Institute for Biomedical Sciences, University of Strathclyde, 27 Taylor Street,
Glasgow, G4 0NR, UK.
g.mcconnell@strath.ac.uk

Allister I. Ferguson
Department of Physics, University of Strathclyde, 107 Rottenrow, Glasgow G4 0NG, UK.

Abstract: Simultaneous stimulated Raman scattering (SRS) and second harmonic generation (SHG) are demonstrated in periodically poled lithium niobate (PPLN). Using a simple single-pass geometry, conversion efficiencies of up to 12% and 19% were observed for the SRS and SHG processes respectively. By changing the PPLN period interacting with the photonic crystal fibre based pump source and varying the PPLN temperature, the SHG signal was measured to be tunable from λ =584 nm to λ =679 nm. The SRS output spectrum was measured at λ =1583 nm, with a spectral full-width at half-maximum of λ =85 nm.

1. Introduction

Extending the spectral coverage of stable laser sources is key to improving the range and efficiency of applications as diverse as optical microscopy, spectroscopy and remote sensing. For this reason, nonlinear optical frequency conversion methods are often used to create coherent sources with emission wavelengths that are difficult or impossible to access with standard laser gain media [1-3]. Stimulated Raman scattering (SRS) is one-such powerful yet simple example of a nonlinear method that exploits the third-order material response to evoke an intensity-dependent Raman shift of the input wavelength. This frequency shift to a longer wavelength increases the spectral range of the existing platform source. We report the application of periodically poled lithium niobate (PPLN) to perform simultaneous SRS and second harmonic generation (SHG) to extend the wavelength range of a soliton self frequency shifted (SSFS) Nd3+:YLF laser. Use of a PPLN crystal provides access to a very high nonlinear gain coefficient for high efficiency of the SRS and SHG processes. In the simple single-pass configuration adopted, conversion efficiencies of 19% and 12% were measured for the SHG and SRS outputs respectively. Changing the interaction period and the temperature of the PPLN crystal created a SHG signal that was tunable over λ=584 nm to λ=679 nm. The concurrently generated SRS output spanned a full-width at half-maximum (FWHM) of λ=85 nm, centred at λ=1583 nm.

2. Background

Periodically poled crystals are invaluable media for performing nonlinear optical frequency conversion as they provide access to high nonlinear coefficients, possess high damage thresholds and have simple phase-matching requirements [4]. The quasi-phase-matching (QPM) procedure typically involves applying a high-magnitude electric field in a predetermined pattern to a ferroelectric material such as lithium niobate, resulting in alternating polarity domain periods of length Λ, which is twice the coherence length for this process. After one coherence length, the wave-vector mismatch Δk is reset to zero by reversing the sign of the nonlinear coefficient, leading to a constructive conversion process. For the specific case of periodically poled lithium niobate (PPLN), use of the d33 tensor component in this arrangement allows second-order nonlinear

coefficients of up to 16 pm/V to be accessed [5]. This is a five-fold increase over the effective nonlinear gain coefficient of bulk lithium niobate using birefringence phase matching. Furthermore, the acceptance bandwidth for QPM structures is typically larger than those for conventionally phase-matched devices since QPM allows the use of the same polarization for the input and generated frequencies [6]. Solid-state nonlinear materials such as PPLN are well-suited to efficiently generating SRS radiation as the nonlinear gain coefficient is higher than in fluid media due to an increase in the concentration of Raman scattering centres [7]. Although there are many reports of SRS in bulk nonlinear materials, reports on SRS in periodically poled materials are currently limited. Pasiskevicius et al [8] described SRS in an optical parametric oscillator (OPO) based on periodically poled KTiOPO4 (PPKTP). PPLN has a substantially higher third-order nonlinear gain coefficient than PPKTP [5, 9] and therefore potentially enables more efficient SRS. The use of a material with a higher nonlinear gain coefficient also means that more efficient single-pass SRS can be performed. Application of this more straightforward experimental strategy circumvents possible stability problems caused by OPO cavity length tolerances.

In a study by Sidorov et al [10], substantial Raman peaks in bulk lithium niobate were observed in the X(ZZ)Y orientation. This is the standard orientation adopted in PPLN crystals, as it provides access to the highest nonlinear coefficient. We therefore employed a PPLN crystal cut in the X(YY)Z plane as a basis for our observations and study of simultaneous SRS and SHG in PPLN. The SRS process is acknowledged to be extremely sensitive to the wavelength of the pump source [8]. We therefore exploit the SSFS effect in photonic crystal fibre (PCF) to create a suitable high peak power source for investigating the SRS process in PPLN. The SSFS occurs when Raman self-pumping of a soliton transfers energy from shorter to longer wavelengths, as described recently by Reid et al [11] in PCF. The overall effect is a nonlinearly dependent red-shift of the pulse centre wavelength, creating a soliton-pulsed laser source emitting at longer wavelengths than the input source.

3. Experiment

The experimental arrangement for instigating SRS and SHG in PPLN involved a horizontally polarised continuous-wave mode-locked Nd3+:YLF laser (Biolight, Coherent) and PCF serving as the platform source, as shown in Fig. 1. The Nd3+:YLF source comprised a picosecond-pulsed laser with an external fiber-grating pulse compressor. The average output power from the compressor was 680 mW. The emission wavelength of the source from the compressor was λ=1047 nm with a 6 nm spectral FWHM, measured using a fibre-coupled spectrometer (Ocean Optics). After compresson, pulses of 400 fs duration were measured using a second harmonic autocorrelator, corresponding to a time-bandwidth product of 0.68. Given the source repetition rate of 120 MHz, the peak power of the source was therefore approximately 14 kW.

Fig 1.

This pump light was propagated through a λ/2 plate that was anti-reflection coated for the pump wavelength. Rotating the half-wave plate in the set-up and hence changing the state of the pump light entering the fibre was used to determine the polarization dependence on the efficiency of the SSFS process. The transmitted light was focused into an 84 cm long section of photonic crystal fibre (PCF) using an aspheric lens of focal length f=+8 mm with a numerical aperture of N.A.=0.5. The average power incident on the PCF was measured to be 480 mW. The PCF used in this investigation (Crystal Fibre A/S) had a hexagonal arrangement of air holes surrounding a 3.5 μm diameter core. The separation between neighbouring air holes was 1.8 ± 0.2 μm, with a pitch of approximately 0.35. This resulted in a high non-linearity fibre with a zero-dispersion wavelength of around λ0=800 nm. At the pump wavelength, the fibre exhibited a low and anomalous dispersion. The transmitted output from the fibre was collimated using another aspheric lens of f=+4.5 mm focal length lens and

N.A.=0.55. Neither the focusing nor collimating aspheric lenses were anti-reflection coated at the pump or SSFS wavelengths and therefore contributed to Fresnel losses. The collimated PCF output was focused using a spherical lens with an anti-reflection coating at λ=1064 nm of focal length f=+40 mm into a plane-faced PPLN crystal (Crystal Technologies). The spotsize within the PPLN was approximately 31 μm, matching the theoretically optimum beam size for second harmonic generation of the SSFS light calculated using the Boyd and Kleinman method [12]. The uncoated PPLN crystal was 0.5 mm-thick and 6.5 mm-long, and was cut along the X(ZZ)Y direction to provide access to the highest nonlinear gain coefficient. The crystal comprised five regular grating periods of Λ = 10 μm to Λ = 12 μm in 0.5 μm increments. This period length was intentionally chosen to maximise SHG of the SSFS output. The crystal was heated in a custom-built oven with 0.2 °C accuracy to 110 °C to minimise photorefractive damage observed at lower temperatures [13]. Fast wavelength changes were made possible by changing the period of the PPLN interacting with the input beam by translating the crystal relative to the source.

4. Results

The total average power measured at the PCF output (transmission) was 211 mW, with the reduction in power attributed to non-optimal and uncoated fibre input coupling optics and PCF loss. The SSFS average power was measured using two long-wave pass interference filters with a total transmission of 35% at λ>1135 nm and a calorimeter.

Fig 2.

At wavelengths longer than λ=1135 nm, with optimum half-wave plate orientation, up to 56 mW of average power was measured, corresponding to a generated average power of 160 mW of frequency shifted light. A relative average power decrease of up to 24% was measured when the half-wave plate was rotated through 90°, as shown in Fig. 2. The maximum conversion efficiency from pump to SSFS radiation was therefore 24%.

Fig 3.

A maximum shift peak at λ=1258 nm with a spectral FWHM of λ=91 nm was measured using a fibre-coupled spectrometer (Hewlett-Packard). Figure 3 shows an example of the recorded trace for 160 mW of SSFS radiation. It was noted that when the pulse duration delivered by the Nd3+:YLF laser was increased by varying the grating spacing in the pulse compressor, the SSFS spectrum became increasingly narrow. This was not symmetric about the peak wavelength. Instead, the longer wavelength components of the SSFS spectrum disappeared. For the remainder of this report, the optimum pulse duration possible from the Nd3+:YLF for maximum average power SSFS generation was employed. In order to determine the pulse duration of the SSFS output from the PCF, a collinear scanning autocorrelator based on two-photon absorption in a biased GaAsP photodiode (Hamamatsu) was used. Pulses of 220 fs FWHM duration were measured, as shown in Fig. 4. Assuming a sech2 pulse shape, this indicated pulses of approximately 140 fs duration. From the spectral and power data, this measured pulse duration results in a time-bandwidth product of 2.47 and a calculated peak power of around 9kW. The SSFS source served as the platform for studying single-pass SRS and SHG in PPLN.

Fig 4.

Collinear SHG of the SSFS source was observed in PPLN. Continuously tunable output from λ=584 nm to λ=679 nm was measured using a fibre-coupled optical spectrometer with a resolution of 1 nm

(Ocean Optics). Temperature tuning the PPLN crystal from 80 °C to 170 °C and changing the PPLN grating period achieved this broad tuning range. Figure 5 shows a typical tuning range measured by varying the PPLN period, at a fixed temperature of 110 °C.

Fig 5.

By changing the PPLN period, the spectral FWHM varied from 2.8 nm to 4.2 nm. An average power maximum at λ=628 ± 3.1 nm of 30 mW was measured using a calorimeter and optical bandpass filter (Chroma), which is 19% efficient conversion from the SSFS source. This correlates with the spectral range of the fundamental SSFS radiation as already described in Fig. 3. Additionally, 39 mW of radiation at λ=1047 nm and 24 mW of radiation at wavelengths longer than λ=1135 nm were measured in crystal transmission. For input pulses of 140 fs duration, the effective crystal length should ideally be sub-mm for maximum second harmonic conversion. However, the application of longer crystals is understood to reduce the threshold and increase the efficiency of the SRS process [7]. For this reason and also for ease of handling, the 6.5 mm long crystal was retained, although we acknowledge that this ultimately reduced the SHG conversion efficiency. Using the SSFS output with a spectral maximum at λ=1258 nm as previously described, at a fixed temperature of 110 °C the SRS spectral maximum was centred at λ=1583 nm (632 cm-1) and had a FWHM of λ=85 nm. This is shown in Fig. 6. The SRS output was observed to propagate noncollinearly with the SSFS input beam at an angle of 28° with a 4 mW threshold, and was therefore easily distinguishable from the generated SHG. With full incident power at the SSFS wavelengths focussed into the PPLN crystal, the power in the SRS spectrum was measured to be 18 mW across the measurable spectral range. The conversion efficiency from SSFS to SRS radiation was therefore calculated to be 12%. The second harmonic of the SRS radiation was also emitted collinearly with the SRS output, at an average power of approximately 1 mW. With the long-wave pass filters placed prior to the PPLN crystal, the SRS signal was reduced in magnitude by almost a factor of two. This was attributed to the 65% decrease in peak power delivered to the PPLN crystal.

Fig 6.

5. Conclusion

In conclusion, we have demonstrated simultaneous SHG and noncollinear SRS in PPLN. This system was based on SSFS in PCF providing the pump wavelengths necessary for the concurrent SHG and SRS. A simple single-pass geometry provided conversion efficiencies of the SSFS radiation to SHG and SRS of 19% and 12% respectively. The SHG process created a tunable source from λ=584-679 nm and the SRS output was at a peak wavelength of λ=1583, with a spectral FWHM of λ=85 nm. With the application of a shorter crystal, the SHG average power would increase but the SRS efficiency would be reduced. One approach to solving this problem would be to power scale the initial laser platform, where the output powers of both the SHG and SRS processes could feasibly reach >100 mW at the novel spectral regions described. Additionally, with increased interest in understanding and exploiting the nonlinear processes in PCF, we envisage the future development of a more efficient SSFS source to study simultaneous SHG and SRS. Applying high-quality anti-reflection coatings to both the PPLN and the aspheric lenses would also increase the efficiency of both the SRS and SHG processes. Future work enabled by this novel wavelength source includes remote sensing of CO2 in the L-band, which extends from 1565 nm to 1620 nm, and further spectroscopy applications.

Acknowledgments

This work was supported by the Royal Society of Edinburgh.

References

1. L.E. Myers and W.R. Bosenberg, ⊠Periodically poled lithium niobate and quasi-phase-matched optical parametric oscillators,⊠ IEEE J. Quantum Electron. 33 1663-1672 (1997).
2. D.W. Chen and K. Masters, ⊠Continuous-wave 4.3-mu m intracavity difference frequency generation in an optical parametric oscillator,⊠ Opt. Lett. 26 25-27 (2001).
3. W.R. Bosenberg, J.I. Alexander, L.E. Myers and R.W. Wallace, ⊠2.5-W, continuous-wave, 629-nm solidstate laser source,⊠ Opt. Lett. 23 207-209 (1998).
4. M.M. Fejer, G.A. Magel, D.H. Jundt and R.L. Byer, ⊠Quasi-phase-matched 2nd harmonic-generation
⊠ Tuning and tolerances,⊠ IEEE J. Quantum Electron. 28 2631-2654 (1992).
5. I. Shoji, T. Kondo, A. Kitamoto, M. Shirane and R. Ito, ⊠Absolute scale of second-order nonlinear-optical
coefficients,⊠ J. Opt. Soc. of Am. B. 14 2268-2294 (1997).
6. F. Laurell, ⊠Periodically poled materials for miniature light sources,⊠ Opt. Mat. 11 235-244 (1999).
7. P.G. Zverev, T.T. Basiev and A.M. Prokhorov, ⊠Stimulated Raman scattering of laser radiation in Raman crystals,⊠
Opt. Mat. 11 335-352 (1999).
8. V. Pasiskevicius, A. Fragemann, F. Laurell, R. Butkus, V. Smilgevicius and A. Piskarskas, ⊠Enhanced stimulated
Raman scattering in optical parametric oscillators from periodically poled KTiOPO4,⊠ App. Phys. Lett. 82 325-327 (2003).
9. I. Jovanovic, J.R. Schmidt and C.A. Ebbers, ⊠Optical parametric chirped-pulse amplification in periodically poled
KTiOPO4 at 1053 nm,⊠ App. Phys. Lett. 83 4125-412 (2003).
10. N.V. Sidorov, M.N. Palatnikov, K. Bormanis and A. Sternberg, ⊠Raman spectra and structural defects of lithium
niobate crystals,⊠ Ferroelectrics 285 685-694 (2003).
11. D.T. Reid DT, I.G. Cormack, W.J. Wadsworth, J.C. Knight, PSJ Russell, ⊠Soliton self-frequency shift effects in
photonic crystal fibre,⊠ J. Mod. Opt. 49 757-767 (2002).
12. G.D. Boyd and D.A. Kleinman, ⊠Parametric interaction of focused Gaussian light beams,⊠ J. App. Phys. 39 3597-3639 (1968).
13. I.A. Ghambaryan, R. Guo, R.K. Hovsepyan, A.R. Poghosyan, E.S. Vardanyan and V.G. Lazaryan, ⊠Periodically poled structures in lithium niobate crystals: Growth and photoelectric properties,⊠ J. Optoelectron. Adv. Mat. 5 61-68 (2003).

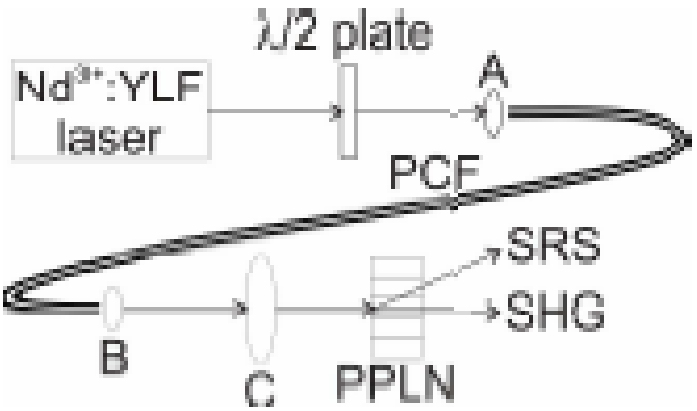

Fig. 1. Experimental set-up. The output of a continuous wave mode-locked Nd 3+ :YLF laser was sent through a half-wave plate into photonic crystal fiber (PCF) using an aspheric lens (A) of focal length f=+8 mm. The fibre output was collimated using another aspheric lens (B) of focal length f=+4.5 mm. Using a spherical lens (C) of focal length f=+40mm, the soliton self- frequency shifted output and the residual pump light was focused into a 6.5 mm long PPLN crystal.

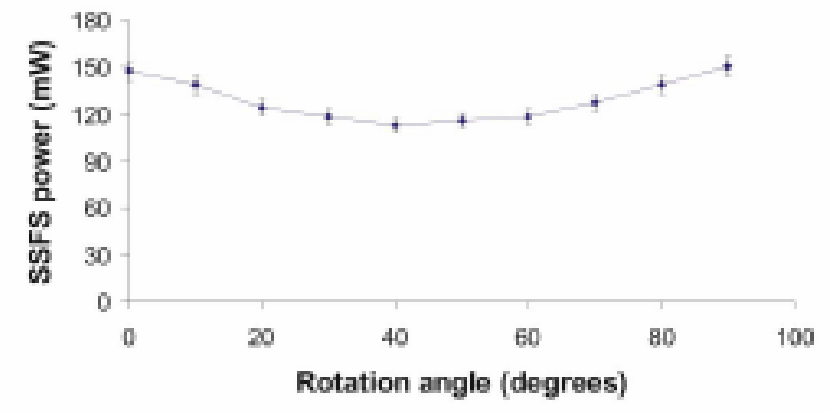

Fig. 2. By rotating the half-wave plate prior to the PCF, a weak polarization dependence of the pump polarization on the SSFS power was observed, with a measured decrease in average power of up to 24%.

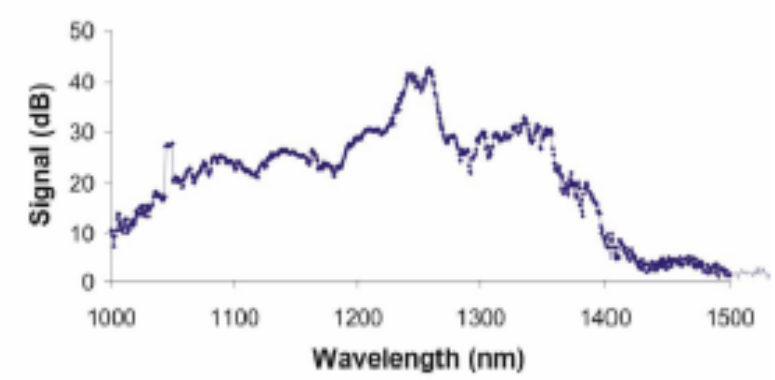

Fig. 3. The SSFS optical spectrum transmitted by the PCF (±1 nm wavelength accuracy, linear scale). The pump laser is evident as a small peak at 1047 nm. The SSFS maximum was measured at 1258 nm.

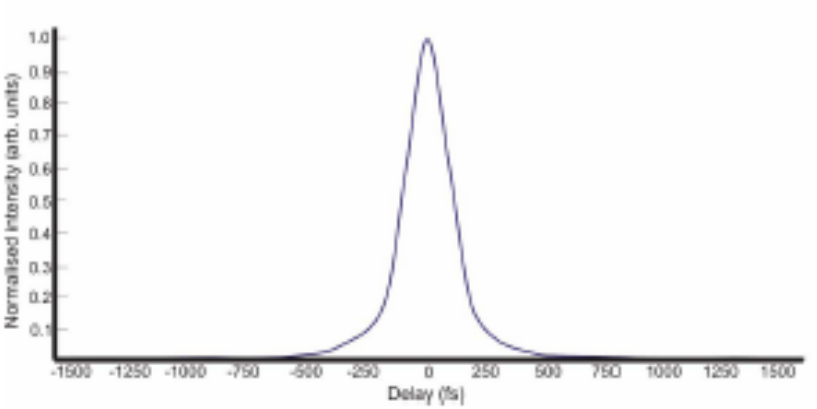

Fig. 4. Two-photon autocorrelation of the SSFS PCF output. The FWHM of the measured pulse was 220 fs. Assuming a sech 2 pulse shape, this corresponded to a pulse width of approximately 140 fs.

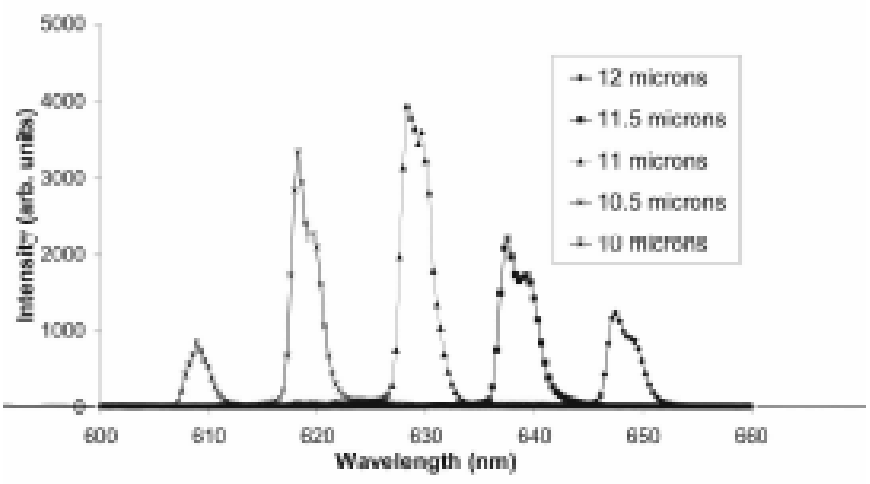

Fig. 5. The SHG spectra as measured at the PPLN output, where the PPLN crystal was held at a fixed temperature of 110 °C. The legend refers to the period length chosen to interact with the input SSFS radiation. The bandwidth of the SHG output varies from 2.8 nm to 4.2 nm.

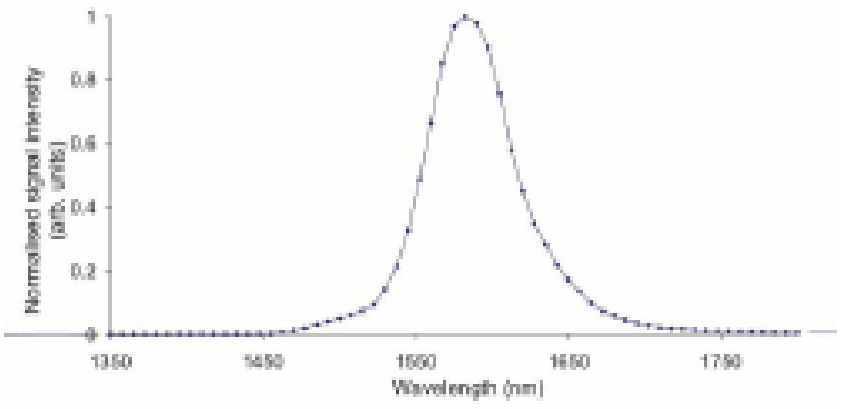

Fig. 6. The SRS spectrum resulting from pumping the PPLN with the SSFS source. The spectral peak was measured at λ =1583 nm, with a λ =85 nm FWHM.